Chemosphere 274 (2021) 129736

Contents lists available at ScienceDirect

Chemosphere

journal homepage: www.elsevier.com/locate/chemosphere

Geochemistry and mineralogy of coal mine overburden (waste): A study towards their environmental implications

Nazrul Islam [a, b], Shahadev Rabha [a, b], K.S.V. Subramanyam [c], Binoy K. Saikia [a, b, *]

[a] Coal & Energy Group, Materials Science and Technology Division, CSIR-North East Institute of Science and Technology, Jorhat, 785006, Assam, India
[b] Academy of Scientific & Innovative Research (AcSIR), Ghaziabad, 201002, India
[c] CSIR- National Geophysical Research Institute, Uppal Road, Hyderabad, 500007, India

HIGHLIGHTS

- Overburdens (coalmine waste) from Northeast (NE) Indian coalfields are studied.
- Advance analytical techniques are applied for chemical analysis of coalmine overburden.
- Concentration of PHEs and REYs in overburden are determined and studied.
- The ecological risk & environmental implications of the trace elements in OB are discussed.

GRAPHICAL ABSTRACT

ARTICLE INFO

Article history:
Received 9 November 2020
Received in revised form
3 January 2021
Accepted 18 January 2021
Available online 25 January 2021

Handling Editor: Martine Leermakers

Keywords:
Open-cast mining
Overburden (OB)
Rare earth elements and yttrium (REY)
Geochemistry
Mineralogy
Ecological risk (Er)
Principal component analysis (PCA)

ABSTRACT

Open-cast mining of coal generates waste material, including rock and soil with different minerals, and traditionally dumped as waste over the valuable lands worldwide. Overburden (OB) is devoid of actual soil characteristics, low micro and macronutrient content, and a sufficient amount of rare earth elements, silicate, sulphate, and clay minerals. This study aimed to determine the geochemistry and mineralogy of OB samples collected from Makum coalfield, Margherita of Northeast (NE) India. The geochemical and mineralogical analyses of overburden (OB) were carried out by using X-ray diffraction (XRD), Fourier transform infrared spectroscopy (FT-IR), High resolution-inductively coupled plasma mass spectrometer (HR-ICP-MS), Field-emission scanning electron microscopy (FE-SEM) techniques. This study shows potentially hazardous elements (PHEs), including Pb, Co Cu, Cr, Ni, and Zn, and their association with minerals observed in OB samples. The major oxides (SiO_2, Al_2O_3, Fe_2O_3, MgO, CaO, K_2O, and Na_2O) are present in all the overburden samples analyzed by the X-ray fluorescence (XRF) technique. Various minerals such as quartz, kaolinite, gypsum, melanterite, rozenite, hematite, and pyrite were identified. The overburden samples contain considerable amounts of rare earth elements and yttrium (REY; as received basis) with an average of 26.3 (ppm). The presence of abundant minerals and REY opens up a new avenue for the gainful and sustainable utilization of such waste materials.

1. Introduction

Coal is considered the world's most abundant fossil fuel and is an chief energy resource used mainly power generation. Generally, in India to produce electricity accounting for, more than 70% of the

* Corresponding author. Coal & Energy Group, Materials Science and Technology Division, CSIR-North East Institute of Science and Technology, Jorhat, 785006, Assam, India.
E-mail addresses: bksaikia@neist.res.in, bksaikia@gmail.com (B.K. Saikia).

https://doi.org/10.1016/j.chemosphere.2021.129736
0045-6535/

total electricity production (Gupta and Paul, 2015; Chikkatur, 2005). Open-cast mining is gradually increasing in the share of coal production. India has large coal reserves and rank fourth among the worldwide identified reserves (Nath et al., 2019). About 17 coalfields are located in India's Northeast (NE) region, and additional l44 major coalfields are located in Indian Peninsula. In India, open-cast mining contributes 80–90% of total coal production, whereas underground mine accounts for 10–20% (https://coal.nic.in/sites/upload_files/coal/files/coalupload/provisional1314_0.pdf). Open-cast mining generates waste material containing rock and soil, along with different types of minerals. This waste material generated during open-cast mining is often termed as overburden (OB) (Prashant et al., 2010). It is reported that the amount of OB is more in open-cast mining than in underground mining processes. Indian Bureau of Mines reported that 7,55,440 ha area is under mining lease, and 5% (about 37,772 ha) is under active mining (Juwarkar and Jambhulkar, 2008). During mining operations in 2001–2002, an overburden of 1870 Mt was removed to produce 623 Mt of coal in India (IBM, 2001). Earlier studies also reported that 4 m^3 of overburden is generated per tonne of coal in open cast mining, and the expected amount of 250 Mt of coal will result in 1000 m^3 overburden. For this amount of mined coal, it is reported that, per year, 60 km^2 of land is degraded in mining activity, and about 75 km^2 is used for dumping external rock, soil, and overburden (Kundu and Ghose, 1997; Juwarkar and Jambhulkar, 2008).

Coal India Limited (CIL) located in the Assam, NE region, has generated more than 1000 ha of OB-disposal land (Gupta and Paul, 2015). The NE region coalfields produce coal and waste materials such as OB with high sulphur (2–12%), mainly in the state of Assam (Dutta et al., 2017). In the Northeastern coalfields: Ledo, Tirap, Tikak, Tipong, and Baragolai are the five major working collieries operated by Coal India Limited. The generated OB is mainly composed of alluvial loose sand, shale, gravel, and sandstone. The sedimentary rocks contain quartz and feldspar as key mineral with different colors (Nath et al., 2019). The mined and rejected sedimentary rock's compressive strength varies from 20 to 170 N/mm2; and its specific gravity and porosity range from 1.85 to 2.7 and 5–20%, respectively as reported by Skarzynska (1995).

The overburden is associated with some potentially toxic elements, and the high amount of sulphur also leads to the formation of highly acidic leachates (Dutta et al., 2017; Baruah et al., 2006; Dowarah et al., 2009). The dumped overburden changes the natural soil topography, generates acid mine water, and prevents natural succession of plant growth, tending to cause soil degradation, soil erosion, and environmental pollution. Earlier studies reported that overburden does not support planting due to the absence of significant minerals or nutrients (Dowarah et al., 2009; Dutta et al., 2017). Physico-chemical characteristics of overburden are area-specific due to different geological deposits of rocks (Archis, 2015; Lovesan et al., 1998).

The main objectives of the present study are as follows: (1) to evaluate the geochemistry and mineralogy of coal-mine overburden samples collected from Ledo and Tirap colliery of Makum Coalfield area of the Northeast region by using different multi-analytical (XRD, FT-IR, FE-SEM, HR-ICPMS) and chemical techniques to understand the REY + Y) potential phases (2) to investigate the concentrations of potentially hazardous elements and REY present in overburden samples, and (3) to examine their occurrence and mutual co-relationship with the help of multivariate statistical analysis (Principal component analysis and Hierarchical clustering analysis).

2. Experimental sections

2.1. Geographical information of the study site

The Makum coalfield is one of the most important coalfields of NE India, extends from 27°15 to 27°25 N latitude and 95°40 to 95°50 E longitude along the outermost flank of the Patkai range. The Makum coalfield, encompassing the open-cast Ledo and Tirap mines and the underground Baragolai, Tikak, and Tipong collieries, consists of separate, tectonic blocks isolated in the Schuppen Belt (Saikia et al., 2016; Sarma, 2013). For the current study, the OB samples were collected from Tirap (OB-1 and OB-2) and Ledo (OB-3 to OB-11) open-cast coal mine areas by using standard methods (ASTM D5633-04). These two collieries are the active and surrounded by rural habitation and agricultural activity or land, tea gardens, and a residential colony. The detailed information of the study area is summarized in Fig. 1. The collected overburden samples were air-dried and ground to a top-size of 0.211 mm and kept in desiccators for characterization and identification of elements and minerals present.

2.2. Proximate analysis of the overburden

The samples (OB) were analyzed to evaluate their chemical properties. Proximate analysis was carried out with the help of a Thermogravimetric analyzer (TGA 701; Leco Corporation, USA) by using a standard method (ASTM D5142-04).

2.2.1. Fourier transform-infra red (FT-IR) spectroscopic analysis

FT-IR spectroscopic analysis was carried out in a Perkin Elmer System 2000 apparatus in the range of 400–4000 cm^{-1}. Samples (OB) were thoroughly mixed with KBr powder in an agate mortar. FT-IR analysis was undertaken using the software spectrum V-3.02 (Version 3.02.01, Perkin Elmer) in advance mode following method reported by Islam et al. (2019).

2.3. X-Ray diffraction analysis

X-Ray Diffraction analysis of the samples was performed in an X-ray diffractometer (Rigako, Ultima IV), adopting the procedure mentioned elsewhere (Rabha et al., 2018). The X-ray diffraction data of the samples were obtained with starting angle set at 2.00° and stopping angle set at 90.00° and step angle 0.02° with a scanning rate of 1 °C/min and target Cu–K α (λ = 1.54056A°). The library database 'RigakuPDXL 1.2.0.1' program was used for the identification of mineral peaks.

2.3.1. Field emission-scanning electron microscopy (FE-SEM) analysis

Field emission-scanning electron microscopy (FE-SEM) images were obtained from an electron microscope (Make: Carl Zeiss Sigma). Energy-dispersive X-ray spectroscopy (EDS) pattern and elemental mapping analysis were also recorded on Oxford X Max 20 equipment attached to the microscope.

2.3.2. X-ray fluorescence spectroscopic analysis

For determination of minor and major oxides in OB samples, the X-ray fluorescence (XRF Model: Pan Analytica Axiom WD-XRF system) method was utilized by following the technique reported by Krishna et al. (2017) at CSIR-NGRI, Hyderabad. Fine powder (0.075 mm) of rock samples and standards (Chinese standard reference materials such as GSR-4 sandstone, and GSR-5, shale)

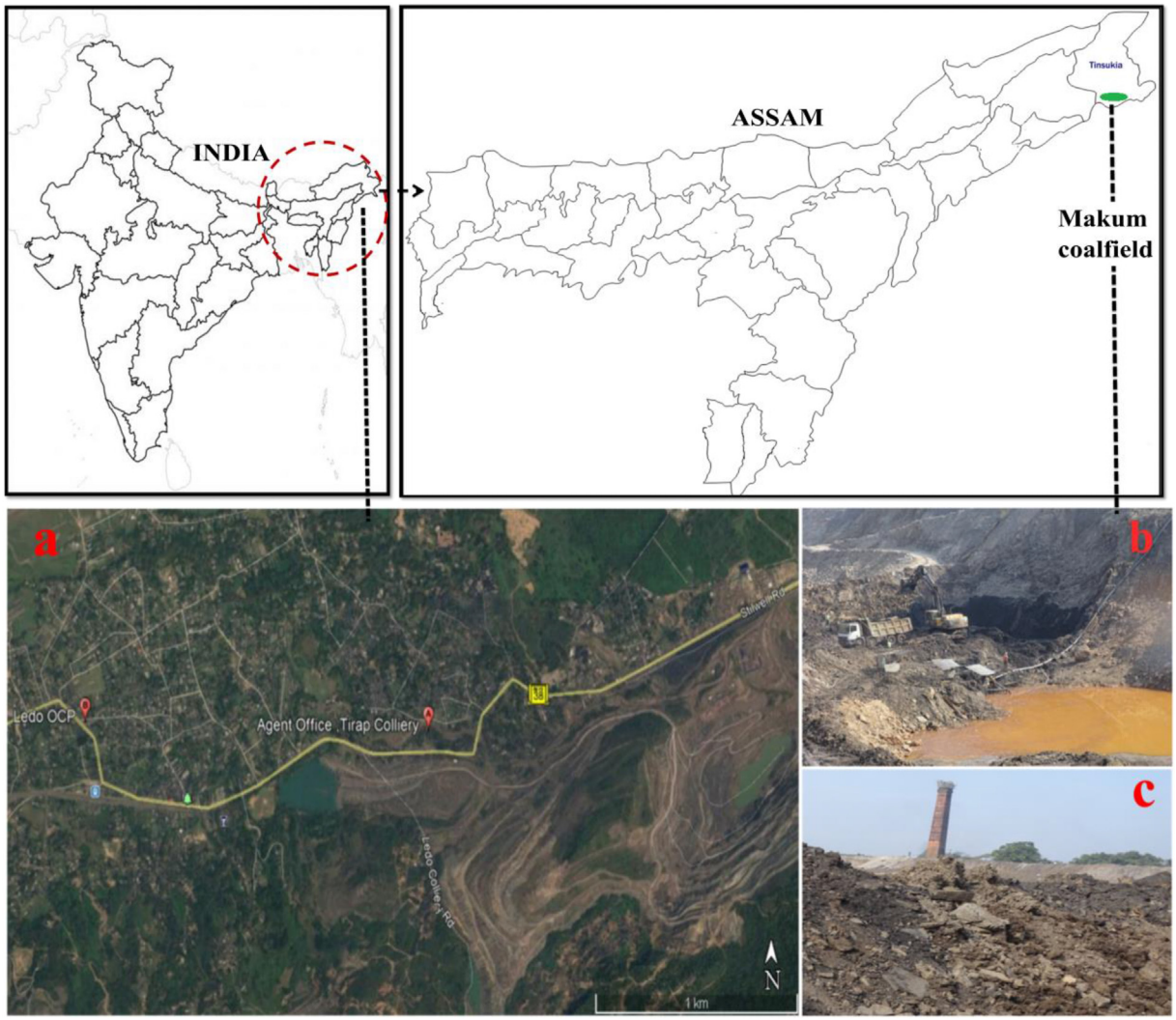

Fig. 1. Location of Ledo and Tirap open-cast mine areas showing the topography and generation of overburden (not in scale).

were prepared as pressed pellets. Major oxides (SiO_2, Al_2O_3, Fe_2O_3, MgO, CaO, K_2O, and Na_2O) and minor oxides (TiO_2, MnO, and P_2O_5) were determined. Loss on ignition (LOI) on these samples were determined by using a high-temperature muffle by heating 1 g of sample in a pure silica crucible at 950 ^{O}C for 1 h.

2.3.3. Inductively coupled plasma-mass spectrometer (ICP-MS) analysis

The trace and REY (REE + Y) concentrations in OB samples were quantified by using a High Resolution Inductively Coupled Plasma Mass Spectrometer (HR-ICP-MS; Nu Instruments Attom®, UK). For this analysis, the samples were digested based on the analytical protocols reported by Satyanarayanan et al. (2018). The same international standard reference materials were used for analytical parameters and instrument calibration methods for trace (Ba, Cu, Cr, Co, Ni, Zn, and Pb) and REY (Sc, V, Ga, Se, Rb, Sr, Y, Zr, Nb, Cs, La, Ce, Pr, Nd, Sm, Eu, Gd, Tb, Dy, Ho, Er, Tm, Yb, Lu, Hf, Ta, Th and U) determination (Satyanarayanan et al., 2018). The analytical precisions for major and minor oxides are ranged between 2 and 4% RSD while those for trace elements and REY range up to 5–7%. REY data are normalized to the Upper Continental Crust (UCC) compositions following Rudnick and Gao (2003).

2.3.4. Environmental implications of trace and REY

2.3.4.1. Enrichment factor analysis. Enrichment Factor (EF) analysis was carried out to assess the elemental enrichment obtained from OB samples. For this study, TiO_2 was considered as reference species for the detection of enrichment and their sources, as suggested in earlier studies (Hussain and Luo, 2020). EF is defined as the double ratio of the concentration of elements (C) present in OB samples to that of reference species (TiO_2) in OB and earth crust (Hussain and Luo, 2020; Islam and Saikia, 2020). It can be calculated by using the following equation:

$$EF = \frac{(Ci/TiO_2)OB}{(Ci/TiO_2)earth\ crust}$$

EF values can be categorized into five categories to detect the enrichment of trace elements and REY. The categories are: reduction to minimal enrichment (EF < 2); moderate (EF = 2–5), significant (EF-5-20), very strong (EF = 20–40) and extreme (EF > 40) (Sutherland, 2000; Islam and Saikia, 2020).

2.3.4.2. Potential ecological risk analysis. The potential ecological risk (PER) analysis was performed to determine the toxicity of metal pollution and associated ecological risk of OB. Based on

toxicological importance, six elements (Cr, Cu, Co, Ni, Zn, and Pb) were used to calculate PER by using the following equation.

$$PER = \sum Er_i = \sum T_i \frac{S_i}{B_i}$$

Where Er_i is the ecological risk factor of the metal (Karina et al., 2019). S_i is the concentration of metal in OB sample, B_i is the background value and T_i is the biological toxicity factor of each element. The B_i and T_i values were used as suggested by Ahamad et al. (2019). The Ecological risk (Er) can be categorized into five category including low risk (Er < 40), moderate (Er = 40–80), considerable (Er = 80–160), high (Er = 160–320), and very high risk (Er ≥ 320) (Ahamad et al., 2019; Karina et al., 2019).

2.4. Multivariate statistical analysis of the elements

Principal Component Analysis (PCA) and Hierarchical clustering analysis (HCA) of elements, including rare earth elements (REY) concentrations of OB, was used to establish a linkage between the produced data or a new set of orthogonal data for correlation analysis. This technique is a widely used statistical multivariate analysis method that reduces and transforms a large number of original data/variables (individual concentration of elements or REY of OB) into smaller variables or uncorrelated latent factor (principal component). The multivariate statistical analysis (PCA and HCA) of the elements present in OB was carried out, as reported elsewhere (Islam and Saikia, 2020; Suman et al., 2016; Islam et al., 2020).

3. Results and discussions

3.1. Physico-chemical properties of coal mine overburden

The proximate analysis was performed to determine the overburden sample's basic chemical properties (OB-1 to OB-11). The summary of the results are shown in Table 1. From this analysis, it was observed that the OB samples of Tirap (OB-1 and OB-2) and Ledo (OB-3 to OB-11) colliery had low moisture contents (0.36–3.36%), volatile matters (5.48–14.6%), and high ash content (72.2–92.9%). The similar high ash content in OB samples was also reported in other studies (Saikia et al., 2015; Dutta et al., 2017). It was also reported that the total sulphur content present in OB samples are lower as compared to coals of these collieries (Dutta et al., 2017 Saikia et al., 2016). This may be due to the association of sulphur with coal in the paleomires during peat formation process (Singh et al., 2013; Singh et al., 2012, 2017a, b).

Table 1
Physico-chemical properties of overburden (as received basis, wt%).

Sample	Moisture	Volatile matter	Ash content	Fixed carbon
OB-1	0.36	10.08	89.56	Nil
OB-2	2.42	9.55	87.23	0.8
OB-3	2.84	13.99	76.07	7.1
OB-4	1.11	6.02	92.87	Nil
OB-5	1.23	6.33	92.44	Nil
OB-6	2.05	9.7	88.25	Nil
OB-7	2.17	7.43	90.4	Nil
OB-8	1.2	5.48	90.68	2.64
OB-9	0.74	6.95	92.31	Nil
OB-10	3.36	8.85	87.52	0.27
OB-11	2.75	14.56	72.19	10.5

3.2. XRD-mineralogy

X-ray diffraction analysis was carried to identify the major minerals of the OB samples. The minerals present in OB samples were summarized in Fig. 2. Minerals observed in XRD spectra of overburden samples are mostly quartz, kaolinite, gypsum, hematite, and calcite. Quartz is observed to be the dominant mineral present in all the overburden samples. The dominance of quartz in these samples implies their origin from basement rocks and may be from siliceous phytoliths within the plant's peat-forming tissues (Saikia et al., 2016; Ward 2002). The overburden of coal seams is lithologically composed of sandstone and shale horizons with cyclic repetitions. In the present case, the overburden samples are dominantly sandstones, as also correlated by their high SiO_2 (58–71 wt%), total alkalies (1.3–4.4 wt%), and Al_2O_3 (15–22 wt%) content as major oxides and correlation of REY trends of shale and sandstone with GSR-4 and GSR-5 reference standards.

3.3. Chemical structure/functional groups in the overburden (OB) samples

Fourier transform-infrared (FTIR) spectroscopy is a powerful technique for characterizing the chemical structure of materials. FT-IR analysis also indicates that the OB samples are composed of silicate minerals (quartz) and clay minerals (montmorillonite and kaolinite), as observed in XRD analysis. The functional groups and minerals were identified for different peaks (see Fig. 3 and Table- 2) based on literature (Saikia et al., 2007; Dutta et al., 2017; Rajak et al., 2020). The absorbance peak ranges from 3600 to 3700 cm^{-1} were observed due to the stretching vibration of N–H functional groups; and OH was attributed to montmorillonite. The peak at 1000 cm^{-1} was observed due to the stretching bands of C–O functional group. The absorption peaks at 910, 793, 690, and 540 cm^{-1}were due to the stretching bands of C–C, Si–O, and OH corresponding to quartz

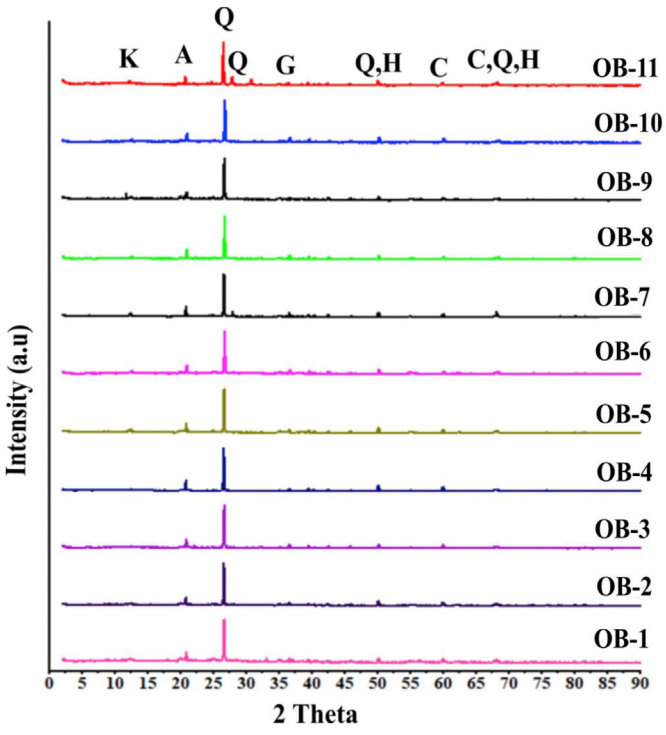

Fig. 2. XRD analysis of overburden samples showing the minerals phases (Q: quartz; H: hematite; I: illite; P: pyrite; C: calcite; K: kaolinite).

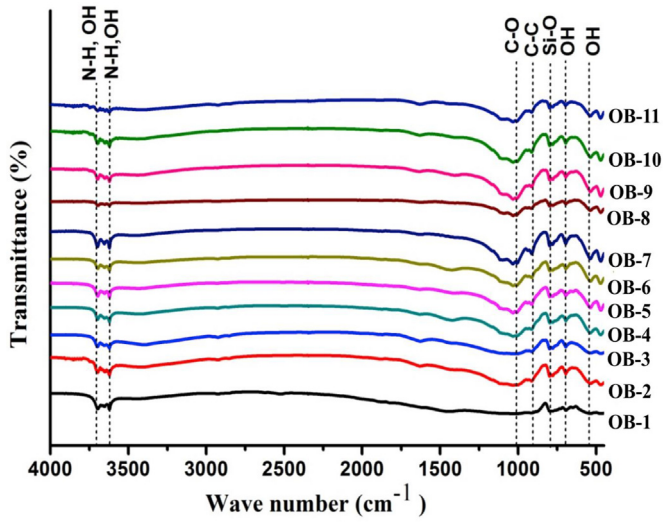

Fig. 3. FTIR analysis of overburden samples showing the presence of functional groups.

Table 2
Possible mineral peaks in FT-IR spectra of OB samples.

Wave number (cm^{-1})	Assignments	Possible minerals
3600–3700	N–H; OH	Montmorllionite, Kaolinite
1000	C–O	Kaolinite
910	C–C	Quartz
793	Si–O	Quartz, Kaolinite
690	O–H	Kaolinite
540	O–H	Kaolinite

and kaolinite (Saikia et al., 2007; Islam et al., 2019). It was reported that the strong bands occur in the region 900-1100 cm^{-1} due to the stretching vibration of Si–O, indicating the presence of quartz (Kumar and Rajkumar 2013).

3.4. Observation from electron beam analysis (FE-SEM)

Overburden particle's morphology and chemical composition would help determine the source of particles and types of minerals. Fig. 4a–f shows the FE-SEM and EDS images of overburden samples. The mineralogical analysis of OB shows the presence of aluminosilicate type minerals such as kaolinite [$Al_2Si_2O_5(OH)_4$] with other minerals containing sulphate minerals such as gypsum [$CaSO_4$.2H2O], melanterite [$FeSO_4.7H_2O$], rozenite [$FeSO_4.4H_2O$]; hematite [Fe_2O_3]and pyrite [FeS_2]. The OB particles occur both in crystalline and amorphous forms associated with different elements, including C, O, Ca, Mg, Fe, K, S, Al, and Ti revealed from EDS analysis. As with much of quartz in coal-mine overburden, the kaolinite may be associated with cell cavities and pores of the coal macerals as filling material (Ward 2002; Kemezys and Taylor, 1964; Balme and Brooks, 1953). During the dominant phase of peat formation, the alteration of detrital sediments led to the distribution of clay minerals in the studied samples (Saikia et al., 2016; Rajak et al., 2020).

The other minerals such as gypsum found to be present in the studied samples and these minerals in addition to the formation from sulphide minerals, may have been deposited within it by the production of gases escaping from the surficial fractures and rock veins of the overburden at the time of rainwater contact with the overburden heap (Masalehdani et al., 2009). However, gypsum could be a precipitation/evaporation product resulting from Ca and SO_4 in coal-mine overburden (Ward, 2002).

3.5. Major oxides, minor oxides, and elemental compositions of the overburden

XRF was used to quantify the major oxides present in the Ledo and Tirap Collieries OB samples (see Table 3). This analysis of the major oxides reveals the presence of high fractions of SiO_2 (58–71%), Al_2O_3 (16–21%), and Fe_2O_3 (0–7%). The higher percentages of SiO_2 and Al_2O_3 confirm the dominance of aluminosilicate type minerals. The rest oxides have significantly low mean weight percentages. The mean weight percentage of LOI is 8.34. Similar results of major oxides were also reported in other studies (Saikia et al., 2015; Ameh, 2019; Zhao et al., 2015). It was also reported that the major oxides like SiO_2, Al_2O_3 and Fe_2O_3 were dominant due to the presence of quartz, clay mineral, and pyrites (Ameh, 2019; Zhao et al., 2015).

The determination of elemental composition in the overburden is growing increasingly important and presents a significant challenge in the management and assessment of environmental issues associated with coal mining activities (Saikia et al., 2015; Finkelman, 1995; Riley et al., 2012; Dai et al., 2004, 2004, 2005, 2012; 2004; Ribeiro et al., 2011). The quantification of OB samples is also important to determine the potential for their economic recovery (Saikia et al., 2015; Seredin et al., 2013; Hower et al., 2013a,b; Dai et al., 2010; Seredin and Dai, 2012, 2014). The concentrations of the trace elements present in overburden samples are summarized in Table 3. Dai et al. (2014) reported that the clay minerals are generally responsible for the occurrence of Zr, Ba, Sr, Hf, V, Ga, Rb, Nb, Cs, U, Th, and the REY in coals. The lithological data of overburden in Makum coalfield (Margherita) shows sandstones with clay, sandy clay, sandy shale, and carbonaceous shale (Saikia et al., 2016; Sharma, 2013). Some factors influence the concentration of elements in the rocks of the OB, including a marine depositional environment, hydrothermal fluids, volcanic ash input, and groundwater (Ren et al., 1999; Dai et al., 2006c, 2008, 2012; Seredin and Finkelman, 2008; Burger et al., 1990, 2000; Zhao et al., 2013; Zhou et al., 2000; Crowley et al., 1989; Hower et al., 1999). The concentrations of Ba and Sr were observed to be higher due to the association of minerals such as calcite or dolomite or phosphates (Ward, 1991; Saikia et al., 2014). Earlier studies reported that U, Cr, and Ni in OB samples are mainly associated with clay minerals and organic matter (Swaine, 2000; Finkelman, 1994). The groundwater is the leading cause for the mobilization and dispersion of these elements which are deposited in the porous overburden rock (Saikia et al., 2016).

3.6. Distribution of rare earth elements (REY) in coal-mine overburden

The rare earth elements (REY) are useful geochemical indicators for sediment provenance due to their stability in nature, as Henderson (1984). The REY along with yttrium (REY, or if yttrium is not included) can be classified into the REY categories include, Heavy (H– Er, Ho, Yb, Tm, and Lu), Medium (M – Gd, Eu, Dy, Tb, and Y), and Light (L- Ce, La, Pr, Nd, and Sm) (Seredin and Dai, 2012). The distribution of in OB samples is illustrated in Table 4. The result shows the L range from 33 to 112 ppm, whereas M varies from 12 to 21 ppm, and H ranges from 9 to 10 ppm. The average REY content in overburden was observed to be 26.33 ppm, which is higher than the earlier studies (Saikia et al., 2016). REY are generally associated with non-coaly material or detritus like shale since REY are hosted by rock-forming minerals like apatite, fluorapatite, allanite, zircon, ilmenite, rutile, etc. (Park et al., 2020). The OB samples under study generally consist of shale/sandstones, including the above rock-forming minerals; a one-to-one comparison is a viable proposition. Hence, similar ash contents of coal are not required to be

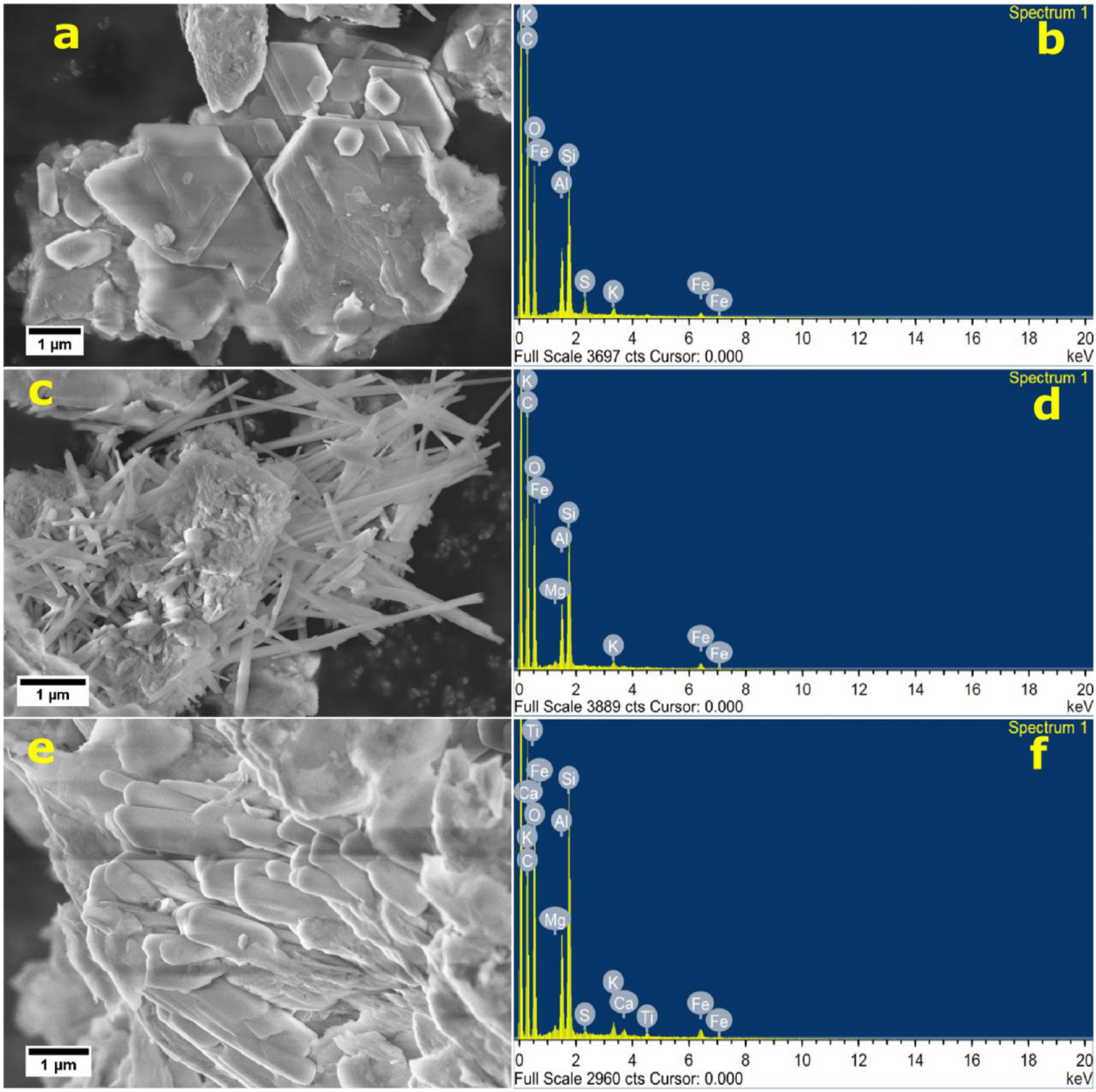

Fig. 4. FE-SEM analysis of coal-mine overburden samples showing the presence of minerals: (a) kaolinite, (c) melanterite and rozenite needles, and (e) gypsum minerals confirmed with the help of SEM-EDS technique showing the presence of chemical compositions (b, d, and f) in OB samples.

Table 3
Major and minor oxides of overburden (wt%).

Oxides	OB-1	OB-2	OB-3	OB-4	OB-5	OB-6	OB-7	OB-8	OB-9	OB-10	OB-11
SiO_2	60.23	60.52	58.97	59.46	62.24	61.37	58.98	65.52	71.64	62.64	61.20
Al_2O_3	18.92	17.28	18.91	19.41	18.22	19.19	18.49	21.83	15.01	16.72	18.35
Fe_2O_3	2.51	8.44	6.86	6.41	5.73	4.61	7.91	1.75	0.79	5.46	6.94
MnO	0.04	0.12	0.04	0.03	0.07	0.05	0.06	0.01	0.01	0.08	0.05
MgO	1.96	1.38	1.02	0.73	1.35	1.53	2.17	0.41	0.36	1.40	1.33
CaO	3.24	0.56	0.30	0.12	0.35	0.80	0.57	0.12	0.05	1.17	0.31
Na_2O	1.70	0.29	0.26	0.36	0.41	1.13	0.42	0.20	0.16	0.36	0.33
K_2O	1.07	1.72	1.95	1.84	1.93	1.29	1.88	1.48	1.22	1.67	1.65
TiO_2	0.73	1.07	1.21	1.15	1.34	0.78	0.92	1.08	0.67	1.18	1.10
P_2O_5	0.12	0.10	0.05	0.04	0.08	0.03	0.10	0.03	0.05	0.09	0.07
LOI	7.50	6.90	10.10	10.30	7.60	8.10	8.12	7.16	9.60	8.80	8.10
Others*	1.98	1.62	0.33	0.15	0.68	1.12	0.38	0.41	0.44	0.43	0.57
Total	**100.00**	**100.00**	**100.00**	**100.00**	**100.00**	**100.00**	**100.00**	**100.00**	**100.00**	**100.00**	**100.00**

(LOI-Loss on ignition; *Calculated by difference from 100%.).

Table 4
Concentrations and distribution of trace elements and REY in the OB samples (ppm).

Elements	OB-1	OB-2	OB-3	OB-4	OB-5	OB-6	OB-7	OB-8	OB-9	OB-10	OB-11	Average
Sc	8.03	12.44	14.05	13.14	10.54	9.53	12.44	13.75	4.71	7.89	13.36	**10.90**
V	68.20	110.06	142.34	130.14	95.88	90.68	115.86	134.69	46.50	71.40	121.45	**102.47**
Cr	65.04	49.08	50.26	49.22	47.98	47.28	50.00	52.82	34.38	39.45	48.40	**48.54**
Co	18.35	21.89	20.33	22.52	17.43	17.91	19.82	16.23	4.31	14.49	20.12	**17.58**
Ni	48.32	38.20	42.04	51.50	29.31	39.30	42.82	41.60	17.68	26.82	43.86	**38.31**
Cu	26.51	21.80	24.40	19.27	31.86	17.06	29.84	27.16	10.28	18.87	24.15	**22.84**
Zn	12.72	11.68	12.42	12.46	7.62	9.17	8.19	10.14	7.73	13.76	8.12	**10.36**
Ga	11.07	14.56	17.62	17.05	13.45	11.82	15.48	18.50	6.47	10.46	16.44	**13.90**
Se	1.07	1.04	1.02	1.04	1.03	1.05	1.00	1.09	1.08	1.04	1.08	**1.05**
Rb	31.48	71.35	90.17	86.33	62.59	41.28	76.15	73.15	31.80	47.93	75.51	**62.52**
Sr	119.87	90.84	187.73	86.15	61.13	72.23	84.89	65.67	55.92	83.33	79.94	**89.79**
Y	15.47	23.65	27.45	19.76	23.41	24.07	23.59	19.78	14.87	16.37	24.35	**21.16**
Zr	147.57	239.41	254.48	258.32	263.84	181.06	263.81	334.00	176.58	177.37	229.33	**229.62**
Nb	6.39	10.59	13.89	12.35	15.18	7.03	10.32	12.81	6.64	11.07	12.03	**10.76**
Cs	2.01	6.53	8.17	7.90	3.82	3.75	8.05	10.98	2.16	2.89	7.37	**5.79**
Ba	352.47	216.33	268.36	206.31	221.02	160.83	224.38	199.03	115.69	212.92	250.58	**220.72**
La	89.55	120.53	122.92	113.68	142.54	98.20	104.46	118.01	69.31	121.60	132.20	**112.09**
Ce	63.56	88.70	91.76	82.41	106.81	66.75	75.85	86.62	53.06	91.19	95.38	**82.01**
Pr	55.83	74.92	79.58	69.46	90.14	66.18	65.20	72.05	46.97	77.58	81.55	**70.86**
Nd	41.47	55.62	61.79	50.04	65.70	49.93	47.84	51.93	34.40	57.01	58.13	**52.17**
Sm	26.66	36.72	41.70	30.62	40.75	33.52	31.21	31.18	22.10	34.16	36.38	**33.18**
Eu	17.06	21.27	25.74	17.88	22.79	21.30	18.30	16.86	14.23	18.81	21.00	**19.57**
Gd	16.57	22.87	26.04	18.85	24.55	22.01	19.93	17.53	13.86	19.91	22.68	**20.44**
Tb	14.30	19.52	22.55	16.52	21.79	19.51	18.24	14.68	12.27	16.06	19.31	**17.70**
Dy	9.57	13.80	16.06	11.72	14.62	13.83	13.60	11.20	8.44	10.43	13.50	**12.43**
Ho	7.55	11.85	14.09	10.24	12.38	11.62	11.49	9.86	7.35	8.48	11.73	**10.60**
Er	6.70	11.05	12.13	9.88	11.14	10.89	11.18	10.74	6.98	7.42	11.52	**9.97**
Tm	7.21	11.94	13.48	11.56	11.81	10.98	12.54	11.86	7.48	8.01	11.89	**10.80**
Yb	6.36	9.70	13.03	9.35	10.58	10.11	11.43	11.03	7.00	8.22	10.81	**9.78**
Lu	6.37	10.44	13.01	9.94	11.29	9.98	12.63	12.99	6.93	7.78	11.03	**10.22**
Hf	1.62	2.12	2.52	2.49	2.79	1.76	2.61	3.31	1.72	1.68	2.26	**2.26**
Ta	0.35	0.78	1.04	0.95	1.15	0.52	0.78	0.96	0.52	0.77	0.95	**0.80**
Pb	18.16	16.45	27.80	14.67	11.69	9.23	13.87	15.48	8.16	20.84	10.66	**15.18**
Th	6.33	9.76	10.13	8.72	10.18	6.92	9.51	11.47	4.71	8.69	11.58	**8.91**
U	1.28	1.67	1.64	1.60	1.35	1.24	1.52	2.02	0.84	1.14	1.84	**1.47**

equated with OB samples. The combustible matter is very minimal in OB samples, similar to mineral matter in coals. It is a simple comparison between two non-combustible materials compositionally co-relatable to shales.

Although several discrimination diagrams are available in the literature, they may not give relevant results due to the unknown and mixed origin of overburden samples. However, the Gondwana and Cenozoic coal basins contain cyclical sandstone sequences and shales with coal seams' intercalations (Valdiya, 2016). In this way, the OB was removed for mining the coal seams, resulting in the mechanical mixing of coarse to very-fine sediments. The samples under present study are compared using critical petrogenetic indicators (using trace elements) to Upper Continental Crust (UCC), Post-Archean Australian Shale (PAAS), as well as with sediments derived from mafic and felsic sources to assess their genesis as well as their lithological characteristics (Table 5). Similarly, major element concentrations in the OB samples are also compared to average shale, sandstone, UCC, PAAS, and North American Shale Composite (NASC) compositions to attest a lithological character (Table 6). Usually, very old overburden dumps result in leaching due to water-soluble chemical constituents (such as calcium, alkalies, large-ion lithophile elements, etc.). In view of this and the fact that overburden samples that are generally exposed for a long-time, the assessment of such parameters is necessary and would help understand geological agents' action. To assess that the OB samples are compared to Miocene Surma sandstones (younger to Tertiary overburden samples) and Ecca Group shale and sandstone (early Permian Karoo group slightly older to present samples),

Table 5
Range of elemental ratios of overburden samples in this study compared to elemental ratios in sediments derived from felsic rocks, mafic rocks, and upper continental crust as well as Surma Group sandstones.

Element ratio	Surma Group Sandstones	Ranges in sediments from felsic sources (Rahman and Suzuki, 2007; Cullers et al., 1988, 1994, 2000; Cullers and Podkovyrov 2000)	Ranges in sediments from mafic sources Rahman and Suzuki (2007); Cullers et al. (1988), 1994, 2000; Cullers and Podkovyrov (2000)	Upper Continental Crust (McLennan (2001); Taylor and McLennan 1985)	PAAS (Condie (1993)	Overburden samples (Present study)
Eu/Eu*	0.63–0.77	0.40–0.94	0.71–0.95	0.63	0.34	0.73–0.82
$(La/Lu)_{CN}$	7.65–11.28	3.00–27.0	1.10–7.00	9.73	9.0	0.83–15.8
La/Sc	2.89–5.01	2.50–16.3	0.43–0.86	2.21	2.375	1.5–2.8
Th/Sc	0.85–2.17	0.84–20.5	0.05–0.22	0.79	0.91	0.5–0.8
La/Co	1.09–7.65	1.80–13.8	0.14–0.38	1.76	1.65	1.0–3.3
Th/Co	0.41–3.25	0.04–3.25	0.04–1.40	0.63	0.63	0.3–1
Cr/Th	4.92–19.77	4.00–15.0	25–500	7.76	7.53	10.6–26

Table 6
A comparison of average chemical composition of the sandstones and shales from the Surma and Ecca Group with published average shales.

Oxides	Ecca Group Baiyegunhi et al. (2017)		Surma Group (Rahman and Suzuki, 2007)	Avg. Shale (Pettijohn 1957)	Avg.Shale (after Turekan and Wedepohl (1961)	UCC (Taylor& McLennan, 1985)	PAAS (Rudnick &. Gao, 2003)	NASC (Gromet et al., 1984)	Present study
(%)	Shale	Sandstone	Sandstone						Avg. coal-mine overburden samples
SiO_2	68.72	76.43	79.3	58.1	58.5	66.6	62.4	64.82	62.1
TiO_2	0.58	0.46	0.5	0.6	0.77	0.64	0.99	0.8	1.0
Al_2O_3	14.26	9.02	8.9	15.4	15	15.4	18.78	17.05	18.4
Fe_2O_3	4.3	3.61	3.4	6.9	4.72	5.04	7.18	5.7	5.2
MnO	0.06	0.07	0.0	Trace	–	0.1	0.11	–	0.1
MgO	1.28	0.59	1.0	2.4	2.5	2.48	2.19	2.83	1.2
CaO	1.57	2.65	0.8	3.1	3.1	3.59	1.29	3.51	0.7
Na_2O	1.63	1.4	1.6	1.3	1.3	3.27	1.19	1.13	0.5
K_2O	3.08	1.57	1.9	3.2	3.1	2.8	3.68	3.97	1.6
P_2O_5	0.17	0.09	0.1	0.2	0.16	0.12	0.16	0.15	0.1

which are summarized in Table 6.

The studied OB samples are matched with the NASC and PAAS shales (see Tables 5 and 6). The OB samples under the present study have moderate SiO_2 contents (58–71%; on average 62%), TiO_2 concentrations averaging 1.0, high Al_2O_3 contents of about 18.4%, and Fe_2O_3 (total Fe as Fe_2O_3) + MgO content of around 6.4 (5.2 + 1.2)%. Compared to the average shale values and NASC, the OB samples are depleted in MgO (1.2%), Na_2O (0.5), K_2O (1.6%), and CaO (0.7%), with little enrichment in Al_2O_3. Thus, geochemically, these samples are classified mainly as shales based on comparing major and minor oxides (Gromet et al., 1984). The low CaO, and alkalies along with high loss on ignition values prompted us to assess the Chemical Index of Alteration, CIA = $[Al_2O_3/(Al_2O_3 + CaO^* + Na_2O + K_2O)] \times 100$ and Chemical Index of Weathering, CIW = $[Al_2O_3/(Al_2O_3 + CaO^* + Na_2O)] \times 100$ values which are 87 and 94, respectively for the studied samples and indicate moderate to high degREY chemical weathering in the source area (Nesbitt and Young, 1982). The CIA is a measure of the ratio of primary minerals and secondary products such as clays. The Chemical index of weathering (CIW) is another reliable source that provides information on the intensity of chemical weathering in the source area (Harnois, 1988). These samples further characterized by slight positive Eu/Eu*. Critical ratios such as $(La/Lu)_{CN}$, La/Sc, Th/Sc, La/Co, Th/Co, Cr/Th with UCC normalized flat REY distribution patterns (Fig. 5) having a little hump at Eu and relative Y and Ho depletion indicate a mixed source (felsic + mafic) for these sediments (Asiedu et al., 2019).

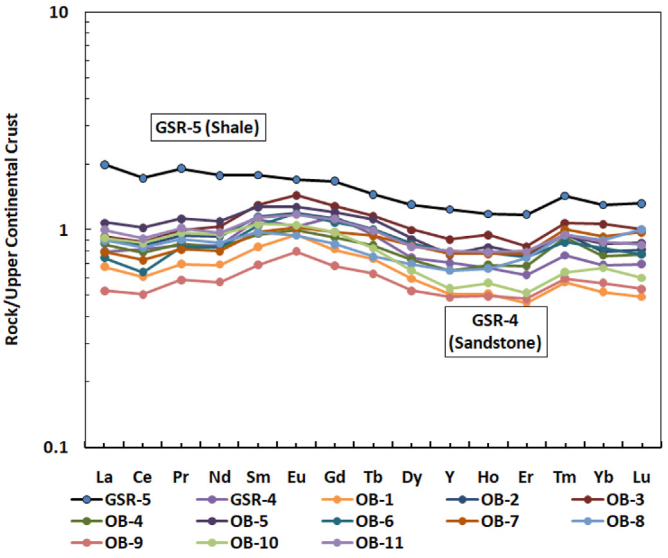

Fig. 5. UCC normalized REY plot for the coal-mine overburden samples.

3.7. Environmental implications of trace and REY

The enrichment factor analysis and potential ecological risk analysis techniques were used to evaluate the potential environmental implications of the elements including REY associated with OB samples. The enrichment factor (EFs) is an important technique to estimate the pollution level and enrichment of an element. The results of the calculated EFs for the elements including REY in OB samples are summarized in Table 7. The enrichment classification revealed that Se, Lu and Tb were very strongly enriched, Pr, Eu, and Tb were significantly enriched and La, Cs, Gd, Er and Tm were moderately enriched in the studied samples. EFs for rest of the elements were observed to be minimal level of enrichment in OB samples of Makum coal fields of NE, India. The significantly enriched elements like Pr, Eu, Sm and Tb are the potential source of monazite mineral as established by Kumari et al. (2015). The enrichment of Se and Lu indicates the source of clay mineral (Mukherjee and Srivastava, 2005). The hazardous elements like Pb, Cu, Cr, Ni, Co, and Zn was observed to be minimal enrichment level in OB samples. It was reported that leaching process leads leach out most of the elements from OB samples of coal mining area (Dutta et al., 2018). But the presence of those hazardous elements indicates the association of pyrite and pyrite oxidation products in OB samples (Vallejuelo et al., 2016).

The potential ecological risk analysis was carried out to determine the biological toxicity of Co, Cr, Cu, Ni, Zn and Pb in OB samples of coal fields of NE India. The results showed that the all the studied elements are under low risk category (see Fig. 6) as suggested by (Ahamad et al., 2019; Karina et al., 2019). None of the elements observed in higher risk category, suggesting limited adverse biological effects (Zhou et al., 2014).

3.8. Multivariate statistical analysis of the elements

Table- 8 shows the Principal Component Analysis (PCA) of elements, including REY. The obtained components are eliminated using an eigenvalue of <1, the first two components are taken and other components are eliminated. Two principal factors explained 69.94% of the total variance of the original data.

The principal factor 1 (PC1) for the concentration of individual elements demonstrates the high loadings of V (0.59), Y (0.69), Nb (0.68), and Ta (0.58) as compared to other elements and accounted for 57.98% of the total variance (Fig. 7). Most of the elements are

Table 7
Enrichment Factor analysis of elements including REY in OB samples (ppm).

Elements	OB-1	OB-2	OB-3	OB-4	OB-5	OB-6	OB-7	OB-8	OB-9	OB-10	OB-11
Sc	0.49	0.75	0.85	0.79	0.64	0.58	0.75	0.83	0.28	0.48	0.81
V	0.76	1.22	1.58	1.44	1.06	1.00	1.28	1.49	0.51	0.79	1.34
Cr	0.85	0.64	0.65	0.64	0.63	0.62	0.65	0.69	0.45	0.51	0.63
Co	0.98	1.16	1.08	1.20	0.93	0.95	1.05	0.86	0.23	0.77	1.07
Ni	0.76	0.60	0.66	0.81	0.46	0.62	0.68	0.66	0.28	0.42	0.69
Cu	0.59	0.48	0.54	0.43	0.71	0.38	0.66	0.60	0.23	0.42	0.53
Zn	0.24	0.22	0.24	0.24	0.14	0.17	0.16	0.19	0.15	0.26	0.15
Ga	0.77	1.02	1.23	1.19	0.94	0.83	1.08	1.29	0.45	0.73	1.15
Se	28.49	27.58	27.16	27.57	27.33	27.92	26.60	28.99	28.57	27.57	28.78
Rb	0.46	1.05	1.33	1.27	0.92	0.61	1.12	1.08	0.47	0.71	1.11
Sr	0.43	0.33	0.67	0.31	0.22	0.26	0.30	0.24	0.20	0.30	0.29
Y	0.62	1.35	1.11	0.80	0.94	0.97	0.95	0.80	0.60	0.66	0.98
Zr	1.19	1.93	2.05	2.08	2.12	1.46	2.12	2.69	1.42	1.43	1.85
Nb	0.42	0.70	0.92	0.82	1.01	0.47	0.69	0.85	0.44	0.74	0.80
Cs	0.89	2.89	3.62	3.50	1.69	1.66	3.56	4.87	0.96	1.28	3.27
Ba	1.10	0.68	0.84	0.65	0.69	0.50	0.70	0.62	0.36	0.67	0.78
La	3.05	4.11	4.19	3.87	4.86	3.35	3.56	4.02	2.36	4.14	4.50
Ce	1.27	1.77	1.83	1.65	2.13	1.33	1.52	1.73	1.06	1.82	1.91
Pr	8.06	10.82	11.49	10.03	13.02	9.56	9.42	10.41	6.78	11.21	11.78
Nd	1.33	1.78	1.98	1.60	2.10	1.60	1.53	1.66	1.10	1.83	1.86
Sm	5.03	6.92	7.86	5.77	7.68	6.32	5.88	5.88	4.16	6.44	6.86
Eu	11.33	14.13	17.10	11.88	15.14	14.15	12.16	11.20	9.45	12.50	13.95
Gd	3.55	4.90	5.58	4.04	5.26	4.72	4.27	3.76	2.97	4.27	4.86
Tb	15.83	21.62	24.96	18.29	24.12	21.60	20.19	16.25	13.58	17.79	21.38
Dy	2.45	3.53	4.10	2.99	3.74	3.53	3.47	2.86	2.16	2.67	3.45
Ho	7.71	12.12	14.40	10.46	12.66	11.88	11.75	10.08	7.51	8.67	11.99
Er	2.54	4.19	4.61	3.75	4.23	4.13	4.24	4.08	2.65	2.82	4.37
Tm	1.84	3.05	3.44	2.95	3.02	2.81	3.21	3.03	1.91	2.05	3.04
Yb	2.64	4.03	5.41	3.88	4.39	4.20	4.75	4.58	2.91	3.41	4.49
Lu	16.93	27.76	34.58	26.42	30.01	26.53	33.58	34.53	18.42	20.67	29.32
Hf	0.72	0.94	1.12	1.11	1.24	0.78	1.16	1.47	0.76	0.74	1.00
Ta	0.23	0.52	0.69	0.63	0.76	0.34	0.52	0.64	0.34	0.51	0.63
Pb	1.72	1.56	2.64	1.39	1.11	0.88	1.32	1.47	0.77	1.98	1.01
Th	0.88	1.35	1.40	1.21	1.41	0.96	1.32	1.59	0.65	1.20	1.60
U	0.63	0.82	0.81	0.79	0.67	0.61	0.75	1.00	0.42	0.56	0.90

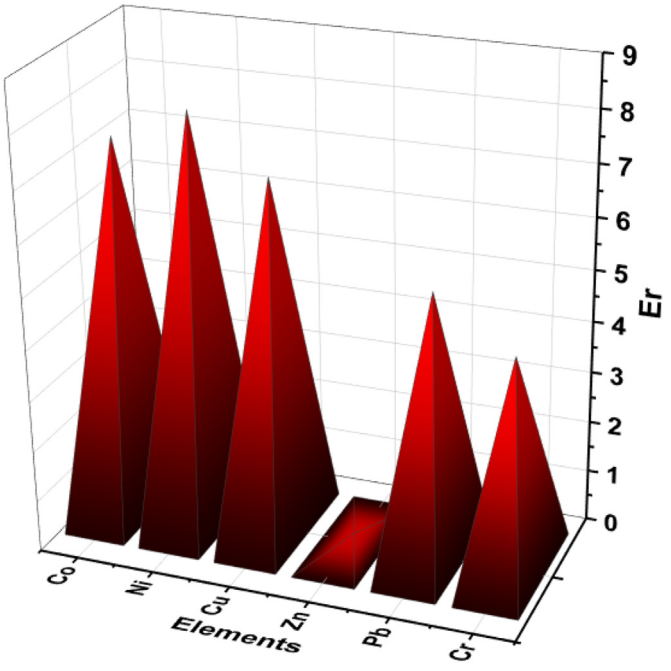

Fig. 6. Ecological risk (Er) analysis of trace elements showing low risk of elements in OB samples.

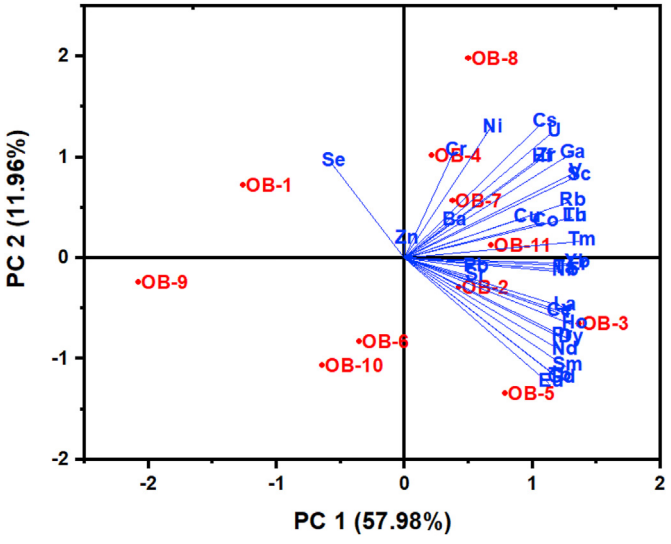

Fig. 7. Principal component analysis showing the bi-plot of the components for the source and relationship of elements.

positively loaded on the both factor PC1 and PC-2, as summarized in Table 8 and Fig. 7. The positive loading of REY indicates that the environment had a low pH, enhancing desorption of REY and also tending to increase the mobility of the elements. High loading of Ta and Nb (high field strength elements) indicates that they may be associated with clay minerals (Saikia et al., 2016).

Hierarchical clustering analysis was also performed to determine the similarities and relationships of trace elements and REY present in overburden samples. Strong hierarchal relations were

Table 8
Matrix of the first two principal components of elements including REY.

Elements	PC-1	PC-2
Sc	0.203	0.175
V	**0.599**	0.181
Cr	0.058	0.227
Co	0.164	0.077
Ni	0.101	0.277
Cu	0.142	0.086
Zn	0.000	0.039
Ga	0.196	0.222
Se	−0.087	0.204
Rb	0.195	0.120
Sr	0.080	−0.040
Y	**0.690**	−0.119
Zr	0.164	0.216
Nb	**0.686**	−0.029
Cs	0.163	0.289
Ba	0.055	0.078
La	0.186	−0.103
Ce	0.180	−0.116
Pr	0.183	−0.169
Nd	0.186	−0.199
Sm	0.190	−0.232
Eu	0.170	−0.268
Gd	0.182	−0.259
Tb	0.180	−0.254
Dy	0.194	−0.172
Ho	0.198	−0.143
Er	0.201	−0.017
Tm	0.206	0.035
Yb	0.201	−0.012
Lu	0.198	0.087
Hf	0.160	0.213
Ta	**0.585**	−0.025
Pb	0.082	−0.021
Th	0.197	0.087
U	0.174	0.268
Eigenvalue	20.29	4.18
Variability (%)	57.98	11.96
Cumulative %	57.98	69.94

observed among the elements Sc, Ga, V, U, Cs, Rb, Er, Tm, Yb, and Lu. Close relationship was also observed between Y with Dy and Ho. The hierarchal relationships of the elements are summarized in Fig. 8. The highly loaded or correlated yttrium (Y) which is also confirmed in PCA analysis indicates that Y is associated with terrigenous input and natural water enriched in Yttrium (Saikia et al., 2016; Dai et al., 2014b). Selenium shows weak relationship with all other elements present in OB samples as confirmed by PCA and HCA analysis (see Figs. 7 and 8). It has also an organic association. Selenium is associated with minerals in coal including pyrite, Ferrosite ($FeSe_2$), and clausthalite (PbSe), which are absorbed in clay or on coal (Mukherjee and Srivastava, 2005).

4. Conclusions

The coal-mine overburden from Makum coalfields North Eeastern region of India) mostly contains minerals including mainly quartz, kaolinite, gypsum, hematite, calcite, melanterite, rozenite, and pyrite confirmed by XRD, FT-IR, and FE-SEM analytical techniques. The higher percentages of oxide minerals such as SiO_2 and Al_2O_3 indicate that the aluminosilicate type minerals dominate the overburden in coal-mine area. The high loading of the principal component of Ta and Nb indicates that they may be associated with clay minerals since clay may be a significant source of Ta and Nb and they are rich in crustal reservoirs. Their presence/loading in overburden samples indicate the mixed sources of their derivation from felsic and mafic rocks as also substantiated by critical REY/HFSE ratios. The Hierarchical clustering analysis (HCA) on the

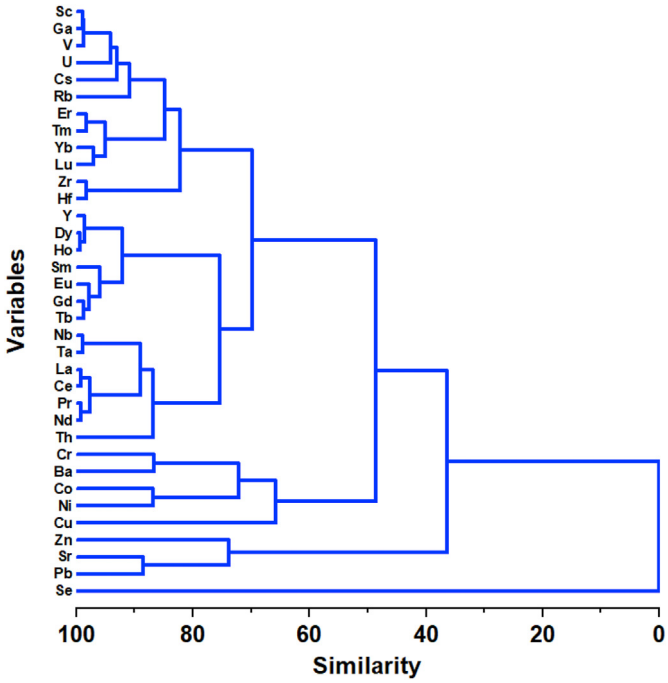

Fig. 8. Hierarchial clustering analysis (HCA) of trace and REY.

elements specifies the association of elements and REY with different types of mineral observed in overburden samples and also shows a significant mutual relationship. The average REY content in overburden samples was 26.3 (ppm), which is to be further studied for optimization and recovery of REY using strong acid or alkali with a large number of samples covering more locations.

Author contribution statement

Nazrul Islam: Methodology, Validation, Investigation, Formal analysis, Writing – original draft. Shahadev Rabha: Methodology, Investigation, Formal analysis. K.S.V. Subramanyam: Methodology, Validation, Formal analysis, Writing – review & editing. Binoy K Saikia: Conceptualization; Methodology; Visualization; Supervision; Writing – review & editing.

Declaration of competing interest

The authors declare that they have no known competing financial interests or personal relationships that could have appeared to influence the work reported in this paper.

Acknowledgments

Authors are thankful to Director (CSIR-NEIST) for his interest to this project. The financial grant received from MoES, India (GPP364) is thankfully acknowledged. Authors are thankful to Prof. Jim Hower and esteemed reviewers for their comments and suggestions to improve the draft.

References

Ahamad, M.I., Song, J., Sun, H., Wang, X., Mehmood, M.S., Sajid, M., Su, P., Khan, A.J., 2019. Contamination level, ecological risk, and source identification of Heavy metals in the hyporheic zone of the weihe river, China. Int. J. Environ. Res. Publ. Health 17 (2020), 1070.
Ameh, E.G., 2019. Geochemistry and multivariate statistical evaluation of major oxides, trace and rare earth elements in coal occurrences and deposits around

Kogi east, Northern Anambra Basin, Nigeria. Int J Coal Sci Technol 6 (2), 260–273.
Asiedu, D.K., Agoe, M., Amponsah, P.O., Nude, P.M., Anani, C.Y., 2019. Geochemical constraints on provenance and source area weathering of metasedimentary rocks from the Paleoproterozoic (~2.1 Ga) Wa-Lawra Belt, southeastern margin of the West African Craton. Geodin. Acta 31 (1), 27–39.
ASTM D5142-04, 2004. Standard Test Methods for Proximate Analysis of the Analysis Sample of Coal and Coke by Instrumental Procedures. ASTM International, West Conshohocken, PA. www.astm.org.
ASTM D5633-04, 2016. Standard Practice for Sampling with a Scoop. ASTM International, West Conshohocken, PA. www.astm.org.
Baiyegunhi, C., Liu, K., Gwavava, O., 2017. Geochemistry of sandstones and shales from the Ecca group, Karoo supergroup, in the eastern cape province of South Africa: implications for provenance, weathering and tectonic setting. Open Geosci. 9, 340–360.
Balme, B.E., Brooks, J.D., 1953. Kaolinite petrifactions in a new south wales coal seam. Aust. J. Sci. 16, 65.
Baruah, B.P., Saikia, B.K., Kotoky, P., Rao, P.G., 2006. Aqueous leaching on high Sulfur Sub-bituminous coals, in Assam, India. Energy Fuels 20 (4), 1550–1555.
Burger, K., Bandelow, F.K., Bieg, G., 2000. Pyroclastic kaolin coal–tonsteins of the upper carboniferous of zonguldak and Amasra, Turkey. Int. J. Coal Geol. 45, 39–53.
Burger, K., Zhou, Y., Tang, D., 1990. Synsedimentary volcanic ash derived illitic tonsteins in Late Permian coal-bearing formations of southwestern China. Int. J. Coal Geol. 15, 341–356.
Chikkatur, A., 2005. Making the best use of India's coal resources. Econ. Polit. Wkly. 40, 5457–5461.
Condie, K.C., 1993. Chemical composition and evolution of the upper continental crust: Contrasting results from surface samples and shales. Chem. Geol. 104 (1–4), 1–37.
Crowley, S.S., Stanton, R.W., Ryer, T.A., 1989. The effects of volcanic ash on the maceral and chemical composition of the C coal bed. Emery Coal Field, Utah. Org. Geochem. 14, 315–331.
Cullers, R.L., 1994. The controls on the major and trace element variation of shales, siltstones, and sandstones of Pennsylvanian-Permian age from uplifted continental blocks in Colorado to platform sediment in Kansas, USA. Cosmochim.Acta. 58, 4955–4972.
Cullers, R.L., Podkovyrov, V.N., 2000. Geochemistry of the Mesoproterozoic Lakhanda shales in southeastern Yakutia, Russia: implications for mineralogical and provenance control and recycling. Precambrian Res. 104, 77–93.
Cullers, R.L., Basu, A., Suttner, L.J., 1988. Geochemical signature of provenance in sand-size material in soil and stream sediments near the Tobacco Root batholiths, Montana, USA. Chem. Geol. 70, 335–348.
Dai, S., Li, D., Ren, D., Tang, Y., Shao, L., Song, H., 2004. Geochemistry of the late Permian No. 30 coal seam, Zhijin Coalfield of Southwest China: influence of a siliceous low temperature hydrothermal fluid. Appl. Geochem. 19, 1315–1330.
Dai, S., Li, D., Chou, C.L., Zhao, L., Zhang, Y., Ren, D., Ma, Y., Sun, Y., 2008. Mineralogy and geochemistry of boehmite-rich coals: new insights from the haerwusu surface mine, jungar coalfield, inner Mongolia, China. Int. J. Coal Geol. 74, 185–202.
Dai, S., Li, T., Seredin, V.V., Ward, C.R., Hower, J.C., Zhou, Y., Zhang, M., Song, X., Song, W., Zhao, C., 2014b. Origin of minerals and elements in the late Permian coals, tonsteins, and host rocks of the Xinde Mine, Xuanwei, eastern Yunnan, China. Int. J. Coal Geol. 121, 53–78.
Dai, S., Ren, D., Chou, C.L., Finkelman, R.B., Seredin, V.V., Zhou, Y., 2012. Geochemistry of trace elements in Chinese coals: a review of abundances, genetic types, impacts on human health, and industrial utilization. Int. J. Coal Geol. 94, 3–21.
Dai, S., Ren, D., Tang, Y., Yue, M., Hao, L., 2005. Concentration and distribution of elements in late permian coals from western guizhou province, China. Int. J. Coal Geol. 61, 119–137.
Dai, S., Seredin, V.V., Ward, C.R., Jiang, J., Hower, J.C., Song, X., Jiang, Y., Wang, X., Gornostaeva, T., Li, X., Liu, H., Zhao, L., Zhao, C., 2014a. Composition and modes of occurrence of minerals and elements in coal combustion products derived from high- Ge coals. Int. J. Coal Geol. 121, 79–97.
Dai, S., Zeng, R., Sun, Y., 2006. Enrichment of arsenic, antimony, mercury, and thallium in a late permian anthracite from xingren, guizhou, southwest China. Int. J. Coal Geol. 66, 217–226.
Dai, S., Zhao, L., Peng, S., Chou, C.L., Wang, X., Zhang, Y., Li, D., Sun, Y., 2010. Abundances and distribution of minerals and elements in high-alumina coal fly ash from the Jungar Power Plant, Inner Mongolia, China. Int. J. Coal Geol. 81, 320–332.
Dowarah, J., Deka Boruah, H.P., Gogoi, J., Pathak, N., Saikia, N., Handique, A.k., 2009. Eco-restoration of a high-sulphur coal mine overburden dumping site in northeast India: a case study. J. Earth Syst. Sci. 118, 597–608.
Dutta, M., Khare, P., Chakravarty, S., Saikia, D., Saikia, B.K., 2018. Physico-chemical and elemental investigation of aqueous leaching of high sulfur coal and mine overburden from Ledo coalfield of Northeast India. Int J Coal Sci Technol 5 (3), 265–281.
Dutta, M., Saikia, J., Taffarel, S.R., Waanders, F.B., de Medeiros, D., Cutruneo, C.M., Saikia, B.K., 2017. Environmental assessment and nano-mineralogical characterization of coal, overburden, and sediment from Indian coal mining acid drainage. Geoscience Frontiers 8, 1285–1297.
Finkelman, R.B., 1995. Modes of occurrence of environmentally sensitive trace elements in coal. In: Swaine, D.J., Goodarzi, F. (Eds.), Environmental Aspects of Trace Elements in Coal. Kluwer Academic Publishing, Dordrecht, pp. 24–50.
Finkelman, R.B., 1994. Mode of occurrence of potentially hazardous elements in coal: levels of confidence. Fuel Process. Technol. 39, 21–34.
Gromet, L.P., Dymek, R.F., Haskin, L.A., Korotev, R.L., 1984. The North American shale composite. Its compilation, major and trace element characteristics. Geochim Cosmochim.Acta. 48, 2469–2482.
Gupta, A.K., Paul, B., 2015. A review on utilisation of coal mine overburden dump waste as underground mine filling material: a sustainable approach of mining. Int. J. Min. Miner. Eng. 6 (2), 172–186.
Harnois, L., 1988. The CIW index: a new chemical index of weathering. Sediment. Geol. 55 (3–4), 319–322.
Henderson, P., 1984. General Geochemical Properties and Abundances of the Rare Earth Elements. Rare Earth Element Geochemistry. Elsevier, Amsterdam.
Hower, J.C., Ruppert, L.F., Eble, C.F., 1999. Lanthanide, yttrium, and zirconium anomalies in the Fire Clay coal bed, Eastern Kentucky. Int. J. Coal Geol. 39, 141–153.
Hower, J.C., Dai, S., Seredin, V.V., Zhao, L., Kostova, I.J., Silva, L.F., Mardom, S.M., Gurdal, G., 2013a. A note on the occurrence of yttrium and rare earth elements in coal combustion products. Coal Combust. Gasification Prod. 5, 39–46.
Hower, J.C., Groppo, J.G., Joshi, P., Dai, S., Moecher, D.P., Johnston, M.N., 2013b. Location of cerium in coal-combustion fly ashes: implications for recovery of lanthanides. Coal Combust. Gasification Prod. 5, 73–78. https://coal.nic.in/sites/upload_files/coal/files/coaluploadprovisional1314_0.pdf.
Hussain, R., Luo, K., 2020. Geochemical evaluation of enrichment of rare-earth and critical elements in coal wastes from jurassic and permo-carboniferous coals in ordos basin, China. Nat. Resour. Res. 29, 1731–1754. https://doi.org/10.1007/s11053-019-09555-9.
Indian Bureau of Mines (IBM), 2001. Annual Report. Ministry of Steel and Mines, Govt. of India.
Islam, N., Saikia, B.K., 2020. Atmospheric particulate matter and potentially hazardous compounds around residential/road side soil in an urban area. Chemosphere 259, 127453.
Islam, N., Dihingia, A., Khare, P., Saikia, B.K., 2020. Atmospheric particulate matters in an Indian urban area: health implications from potentially hazardous elements, cytotoxicity, and genotoxicity studies. J. Hazard Mater. 384, 121472.
Islam, N., Rabha, S., Silva, L.F.O., Saikia, B.K., 2019. Air quality and PM10-associated poly-aromatic hydrocarbons around the railway traffic area: statistical and AirMass trajectory approaches. Environ. Geochem. Health 41 (5), 2039–2053.
Juwarkar, A.A., Jambhulkar, H.P., 2008. Phytoremediation of coal mine spoil dump through integrated biotechnological approach. Bioresour. Technol. 99, 4732–4741.
Karina, C.G., Maria, A.O., Diana, B.Q., Jesus, D.R., Jesus, O.V., 2019. Environmental risks from trace elements in sediments from Cartagena Bay, an industrialized site at the Caribbean. Chemosphere 242, 125173.
Kemezys, M., Taylor G, H., 1964. Occurrence and distribution of minerals in some Australian coals. J. Inst. Fuel 37, 389–397.
Krishna, A.K., Murthy, N.N., Govil, P.K., 2007. Multielement analysis of soils by wavelength dispersive X-ray fluorescence spectrometer. Spectroscopy (Glos.) 28 (6), 202.
Kumar, R.S., Rajkumar, P., 2013. Characterization of minerals in air dust particles in the state of Tamilnadu, India through ftir spectroscopy. Atmos. Chem. Phys. 13, 22221–22248.
Kumari, A., Panda, R., Jha, M.K., Kumar, J.R., 2015. Process development to recover rare earth metals from monazite mineral: a review. Miner. Eng. 79, 102–115.
Kundu, N.K., Ghose, M.K., 1997. Shelf life of stockpiled topsoil of an open-cast coal mine. Environ. Conserv. 24 (1), 24–30.
Lovesan, V.J., Kumar, N., Singh, T.N., 1998. Effect of the bulk density on the growth and biomass of the selected grasses over overburden dumps around coal mining areas. In: Proceedings of the 7th National Symposium on Environment. Dhanbad, Jharkhand, India, pp. 182–185.
Masalehdani, M.N.N., Mees, F., Dubois, M., Coquinot, Y., Potdevin, J.L., Fialin, M., Blanc-Valleron, M.M., 2009. Condensate minerals from a burning coal-waste heap in Avion, Northern France. Can. Mineral. 47, 865–884.
McLenan, S.M., 2001. Relationship between the trace element composition of sedimentary rocks and upper continental crust. G-cubed 2.
Mukherjee, S., Srivastava, S.K., 2005. Trace elements in high-sulfur Assam coals from the Makum coalfield in the northeastern region of India. Energy Fuels 19, 882–891.
Nath, B., Chawla, S., Gupta, R.K., 2019. A Study on Utilization of Mine Overburden as a Replacement of Base and Sub-base Layers on Rural Roads. Springer Nature. https://doi.org/10.1007/978-3-319-95750-0_7.
Nesbitt, H.W., Young, G.M., 1982. Early Proterozoic climates and plate motions inferred from major element chemistry of lutites. Nature 299, 715–717.
Park, S., Kim, M., Lim, Y., Yu, J., Chen, S., Woo, S.W., Yoon, S., Bae, S., Kim, H.S., 2020. Characterization of rare earth elements present in coal ash by sequential extraction. J. Hazard Mater. 402, 123760.
Pettijohn, F.J., 1957. Sedimentary Rocks, second ed. Harper and Row, New York, p. 718pp.
Prashant, Mr, Ghosh, C.N., Mandal, P.K., 2010. Use of crushed and washed overburden for stowing in underground mines, a case study'. J. Mine Met. Fuel 58 (1–2), 7–12.
Rabha, S., Saikia, J., Subramanyam, K.S.V., Hower, J.C., Hood, M.M., Khare, P., Saikia, B.K., 2018. Geochemistry and nano-mineralogy of feed coals and their coal combustion residues from two different coal-based industries in Northeast India. Energy Fuels 32 (3), 3697–3708.
Rahaman, M.J.J., Suzuki, S., 2007. Geochemistry of sandstones from the Miocene

Surma group, Bengal basin, Bangladesh: implications for provenance, tectonic setting and weathering. Geochem. J. 41, 415–428.
Rajak, P.K., Singh, V.K., Singh, Asha Lata, Kumar, N., Kumar, O.P., Singh, V., Kumar, A., Rai, Ankita, Rai Shweta, Naik, A.S., Singh, P.K., 2020. Study of minerals and selected environmentally sensitive elements in Kapurdi lignites of Barmer Basin, Rajasthan, Western India: implications to environment. Geosci. J. 24 (4), 441–458. https://doi.org/10.1007/s12303-019-0029-4.
Ren, D., Zhao, F., Wang, Y., Yang, S., 1999. Distribution ofminor and trace elements in Chinese coals. Int. J. Coal Geol. 40, 109–118.
Ribeiro, J., Valentim, B., Ward, C.R., Flores, D., 2011. Comprehensive characterization of anthracite fly ash from a thermo-electric power plant and its potential environmental impact. Int. J. Coal Geol. 86, 204–212.
Riley, K.W., French, D.H., Farrell, O.P., Wood, R.A., 2012. Huggins F E. Modes of occurrence of trace and minor elements in some Australian coals. Int. J. Coal Geol. 94, 214–224.
Rudnick, R.L., Gao, S., 2003. Composition of the continental crust. In: Holland, H.D., Turekian, K.K. (Eds.), Treatise on Geochemistry, vol. 3. Elsevier-Pergamon, pp. 1–64.
Saikia, B.K., Boruah, R.K., Gogoi, P.K., 2007. XRD and FT-IR investigations of subbituminous Assam coals. Bull. Mater. Sci. 30 (4), 421–426.
Saikia, B.K., Saikia, A., Choudhury, R., Xie, P., Liu, J., Das, T., Dekaboruah, H.P., 2016. Elemental geochemistry and mineralogy of coals and associated coal mine overburden from Makum coalfield (Northeast India). Environ Earth Sci 75, 660.
Saikia, B.K., Ward, C.R., Oliveira, M.L.S., Hower, J.C., Baruah, B.P., Braga, M., Silva, L.F., 2014. Geochemistry and nano-mineralogy of two medium-sulfur northeast Indian coals. Int. J. Coal Geol. 121, 26–34.
Saikia, B.K., Ward, C.R., Oliveira, M.L.S., Hower, J.C., De Leao, F., Johnston, M.N., O'Bryan, A., Sharma, A., Baruah, B.P., Silva, L.F.O., 2015. Geochemistry and nano-mineralogy of feed coals, mine overburden, and coal-derived fly ashes from Assam (North-east India): a multi-faceted analytical approach. Int. J. Coal Geol. 137, 19–37.
Sarmah, R.K., 2013. Study of the maceral composition and coal facies of the oligocene coals in Makum coalfield, Upper Assam, India. Indian J. Appl. Res. 3 (6), 281–285.
Satyanarayanan, M., Balaram, V., Sawant, S.S., Subramanyam, K.S.V., Vamsi Krishna, G., Dasaram, B., Manikyamba, C., 2018. Rapid determination of s, PGEs, and other trace elements in geological and environmental materials by high resolution inductively coupled plasma mass spectrometry. Atom. Spectros 39 (1), 1–15.
Seredin, V.V., Finkelman, R.B., 2008. Metalliferous coals: a review of the main genetic and geochemical types. Int. J. Coal Geol. 76, 253–289.
Seredin, V.V., Dai, S., 2012. Coal deposits as potential alternative sources for lanthanides and yttrium. Int. J. Coal Geol. 94, 67–93.
Seredin, V.V., Dai, S., 2014. The occurrence of gold in fly ash derived from high-Ge coal. Miner. Deposita 49, 1–6.
Seredin, V.V., Dai, S., Sun, Y., Chekryzhov, I.Y., 2013. Coal deposits as promising sources of rare metals for alternative power and energy-efficient technologies. Appl. Geochem. 31, 1–11.
Singh, A.K., Singh, M.P., Singh, P.K., 2013. Petrological investigations of Oligocene coals from foreland basin of northeast India. Energy Explor. Exploit. 31 (6), 909–936.
Singh, P.K., Singh, M.P., Singh, A.K., Naik, A.S., 2012. Petrographic and geochemical characterization of coals from Tiru valley, Nagaland, NE India. Energy Explor. Exploit. 30 (2), 171–192.
Singh, P.K., Singh, V.K., Singh, M.P., Rajak, P.K., 2017a. Understanding the paleomires of eocene lignites of Kachchh basin, Gujarat (western India): petrological implications. International Journal of Coal Science & Technology 4 (2), 80–101.
Singh, P.K., Singh, V.K., Singh, M.P., Rajak, P.K., 2017b. Paleomires of eocene lignites of Bhavnagar, Saurashtra basin (Gujarat), western India: petrographic implications. J. Geol. Soc. India 90, 9–19.
Skarzynska, K.M., 1995. Reuse of coal mining wastes in civil engineering part. Waste Manag. 15 (2), 83–126.
Suman, S., Sinha, A., Tarafdar, A., 2016. Polycyclic aromatic hydrocarbons (PAHs) concentration levels, pattern, source identification and soil toxicity assessment in urban traffic soil of Dhanbad, India. Sci. Total Environ. 545–546, 353–360.
Sutherland, R.A., 2000. Bed sediment-associated trace metals in an urban stream, Oahu, Hawaii. Environ. Geol. 39, 611–627.
Swaine, D.J., 2000. Why trace elements are important. Fuel Process. Technol. 65, 21–66.
Taylor, S.R., McLennan, S.M., 1985. The Continental Crust: its Composition and Evolution. Blackwell Scientific Publications, p. 312.
Turekan, K.K., Wedepohl, K.H., 1961. Distribution of the elements in some major. Units of the Earth's crust. Geol. Soc. Am. Bull. 72, 175–191.
Valdiya, K.S., 2016. Tertiary basins: along coasts and offshore. In: The Making of India. Society of Earth Scientists Series. Springer, Cham. https://doi.org/10.1007/978-3-319-25029-8_20.
Vallejuelo, S.F.O., Gredilla, A., Boit, K., Teixeira, E.C., Sampaio, C.H., Madariaga, J.M., Silva, L.F.O., 2016. Nanominerals and potentially hazardous elements from coal cleaning rejects of abandoned mines: environmental impact and risk. Chemosphere 1–9.
Ward, C.R., 1991. Mineral matter in low-rank coals and associated strata of the Mae Moh basin, northern Thailand. Int. J. Coal Geol. 17, 69–93.
Ward, C.R., 2002. Analysis and significance of mineral matter in coal seams. Int. J. Coal Geol. 50, 135–168.
Zhao, L., Ward, C.R., French, D., Graham, I.T., 2013. Mineralogical composition of late permian coal seams in the songzao coalfield, southwestern China. Int. J. Coal Geol. 116–117, 208–226.
Zhou, C.C., Liu, G.J., Wu, D., Fang, T., Wang, R.W., Fan, X., 2014. Mobility behavior and environmental implications of trace elements associated with coal gangue: a case study at the Huainan coalfield in China. Chemosphere 95, 193–199.
Zhao, L., Ward, C.R., French, D., Graham, I.T., 2015. Major and trace element geochemistry of coals and intra-seam claystones from the Songzao Coalfield, SW China. Minerals 5, 870–893.
Zhou, Y., Bohor, B.F., Ren, Y., 2000. Trace element geochemistry of altered volcanic ash layers (tonsteins) in Late Permian coal-bearing formations of eastern Yunnan and western Guizhou Province, China. Int. J. Coal Geol. 44, 305–324.